

Improved noninterferometric test of collapse models using ultracold cantilevers

A. Vinante,^{1,*} R. Mezzena,² and P. Falferi¹

¹*Istituto di Fotonica e Nanotecnologie, CNR - Fondazione Bruno Kessler, I-38123 Povo, Trento, Italy.*

²*Dipartimento di Fisica, University of Trento, I-38123 Povo, Trento, Italy.*

(Dated: November 30, 2016)

Spontaneous collapse models predict that a weak force noise acts on any mechanical system, as a consequence of the collapse of the wave function. Significant upper limits on the collapse rate have been recently inferred from precision mechanical experiments, such as ultracold cantilevers and the space mission LISA Pathfinder. Here, we report new results from an experiment based on a high Q cantilever cooled to millikelvin temperature, potentially able to fully probe the Adler parameter range for the continuous spontaneous localization (CSL) model. High accuracy measurement of the cantilever thermal fluctuations reveal a nonthermal force noise of unknown origin. This excess noise is compatible with previous bounds on the CSL collapse rate, allowing to significantly extend the exclusion region. Several physical mechanisms able to explain the observed excess noise have been ruled out.

PACS numbers: 03.65.Ta, 05.40.-a, 07.10.Cm, 42.50.Wk

Spontaneous wave function collapse models [1–4] are stochastic modifications of standard quantum mechanics, which have been introduced as a possible solution of the measurement problem. According to such models, the stochastic collapse of the wavefunction is a dynamical process which naturally breaks the quantum superposition principle. The process would occur in atomic systems on a very long timescale, practically unobservable, so that standard quantum mechanics would hold strictly. However, scaling of the collapse rate with the size of the system would lead to a rapid localization of any macroscopic system, and to the emergence of the definiteness of the classical everyday world.

Here we consider the Continuous Spontaneous Localization (CSL) model [2]. CSL is the standard and more general collapse model and has been extensively reviewed in many recent papers [3, 4]. It is characterized by two phenomenological constants, a collapse rate λ and a length r_C , which characterize respectively the intensity and the spatial resolution of the spontaneous collapse. The conservative value for the collapse rate suggested by Ghirardi, Rimini and Weber [1, 2] is $\lambda \simeq 10^{-16} \text{ s}^{-1}$ at $r_C = 10^{-7} \text{ m}$, and is obtained by imposing the collapse to be effective at macroscopic human scale. A collapse rate $10^{9\pm 2}$ times larger has been suggested by Adler [5], motivated by the requirement of making the wave-function collapse effective at mesoscopic level.

Direct laboratory tests based on quantum superposition experiments are currently able to set limits on λ at level of 10^{-6} s^{-1} [6–8]. It has been suggested that much stronger bounds can be set by indirect noninterferometric tests based on mechanical systems [9–16]. Relevant mechanical bounds on λ at level of 10^{-8} s^{-1} for $r_C = 10^{-7} \text{ m}$ have been recently set by cantilever-based experiments [17], cold atoms [18] and the space-based experiment LISA Pathfinder [19]. Stronger bounds, albeit less robust to variations on the model, especially under

Adler assumptions, are set by spontaneous emission of X-rays [20].

Here, we report on a improved version of the cantilever experiment, potentially able to probe collapse rates 1-2 orders of magnitude lower than in previous works, thereby excluding the Adler parameters. Unlike in the previous cantilever experiment [17], we find evidence of a nonthermal excess noise of unknown origin. The noise is compatible with previous bounds, allowing to set stronger limits on λ .

The scheme of our experiment is similar to the one described in Ref. [17] and is shown in Fig. 1. A cantilever with a spherical ferromagnetic load is continuously monitored by a SQUID. The displacement x is converted into magnetic flux by a linear coupling $\Phi_x = d\Phi/dx$ which depend on the magnet position and orientation. A novel feature is that the mechanical quality factor Q is much higher than in previous experiments, and heavily temperature dependent. Moreover, we observe a dynamical SQUID-induced magnetic spring effect, analog to optical spring effects in optomechanics, which modifies the quality factor from its intrinsic value Q to an apparent value Q_a [21]. To account for this new feature, we seek a strategy to directly measure the effective force noise acting on the resonator, rather than the mean energy which may be affected by the dynamically-modified quality factor Q_a . To this end, let us consider the Lorentzian spectral density associated with the cantilever displacement fluctuations:

$$S_x = \left(\frac{S_{f0}}{k^2} + \frac{4k_B T}{k\omega_0 Q} \right) \frac{f_0^4}{(f_0^2 - f^2)^2 + \left(\frac{ff_0}{Q_a} \right)^2} \quad (1)$$

Here, $f_0 = \omega_0/2\pi$ is the resonant frequency, k is the spring constant, k_B the Boltzmann constant. In general, dynamical magnetic spring effects will affect only the denominator of the resonant term. Instead, the amplitude of the Lorentzian curve is independent of Q_a and provides

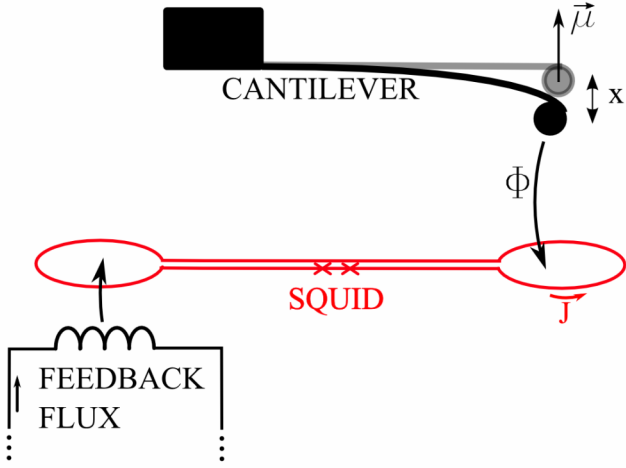


FIG. 1: Simplified measurement scheme. The fundamental bending mode of a cantilever loaded with a ferromagnetic microsphere with magnetic moment μ is continuously monitored by a SQUID susceptometer. The SQUID measures the magnetic flux $\Phi = \Phi_x x$ coupled by the displacement x of the magnetic particle and is operated in flux locked loop (feedback electronics is not shown for simplicity). The flux-dependent circulating current J , combined with finite feedback gain, causes a dynamical magnetic spring effect which modifies the apparent quality factor of the cantilever.

a direct measurement of the force noise. In particular, the thermal force noise term is proportional to T/Q , where Q is the intrinsic quality factor. CSL would cause a white force noise S_{f_0} independent of T/Q . The same effect is actually produced by any excess nonthermal noise. The maximum nonthermal force noise compatible with the experiment can be used to exclude parameter regions in the CSL parameter space. This requires modeling the CSL force acting on the continuous mechanical resonator, exactly as done in Ref. [17].

The mechanical resonator in our setup is a commercial tipless AFM silicon cantilever, with size $450 \times 57 \times 2.5 \mu\text{m}^3$ and stiffness $k = 0.4 \text{ N/m}$. A hard ferromagnetic microsphere (radius $R = 15.5 \mu\text{m}$, density $\rho = 7.43 \text{ kg/m}^3$) is glued to the cantilever free end and magnetized. The microsphere has a twofold function. It increases the cross-section to the CSL field, which scales as ρ^2 [17], while at the same time enabling a straightforward detection by means of a nearby SQUID susceptometer. The SQUID is gradiometric and comprises two distant loops with radius $R_S = 10 \mu\text{m}$ [22]. The particle is aligned above the first loop at a height $h \simeq 40 \mu\text{m}$, with the motion of the first flexural mode orthogonal to the SQUID plane. The SQUID is operated in two-stage flux-locked-loop configuration with the feedback applied to the second loop. This geometry strongly suppresses direct coupling between the feedback signal and the cantilever.

The cantilever-SQUID system is enclosed in a copper box, suspended above the mixing chamber plate of

a pulse-tube dilution refrigerator (Janis Jdry-100-Astra) by means of a two-stage suspension system. The measured mechanical attenuation is higher than 80 dB at the cantilever frequency. The temperature of the mixing chamber is measured by a Ruthenium oxide thermometer calibrated against a superconducting reference point thermometer. The temperature of the SQUID box stage, measured in a subsequent run by a SQUID noise thermometer, is found to be consistent with the mixing chamber thermometer.

The resonant frequency of the fundamental mode of the cantilever is $f_0 = 8173.4 \text{ Hz}$. The actual mechanical quality factor Q_a is determined by ringdown measurements. The dynamical magnetic spring effect depends on the SQUID working point and scales as $1/|G|$ where G ($|G| \gg 1$) is the open loop gain of the feedback electronics. Specifically, we expect a linear dependence of the actual quality factor Q_a as $1/Q_a = 1/Q + c/|G|$, where Q is the intrinsic quality factor and $c/|G|$ is the SQUID dynamical effect. In fact, for infinite feedback gain the SQUID working point would not change any more in response to an input flux, and dynamical effects would be fully suppressed. The expected behaviour is experimentally observed by varying the gain $|G|$, and allows to infer the intrinsic quality factor Q . The whole measurement procedure is repeated at each temperature T .

The measured intrinsic Q is of the order of 6×10^5 at temperature of the order of 1 K, and is observed to increase roughly as $1/T$ upon reducing temperature below $T = 500 \text{ mK}$, approaching $Q \simeq 10^7$ at $T \simeq 20 \text{ mK}$. This behaviour is consistent with measurements performed with the SQUID weakly coupled, and is reminiscent of two-level systems dissipation [23]. Standard glassy two-level systems in a 2 nm amorphous oxide layer on the cantilever surface are able to explain the observed effect quantitatively.

The noise is measured by acquiring and averaging spectra of the SQUID signal, calibrated as magnetic flux, with typical integration time of 800 – 1200 seconds. Before measuring noise and quality factor, the system is let thermalize for at least 3 hours, with the temperature actively stabilized by a PID controller. During the noise measurement the pulse tube is switched off. Examples of averaged flux noise spectra at three representative temperatures are shown in Fig. 2. The spectra are fitted with the curve:

$$S_\Phi = A + \frac{B f_0^4 + C (f^2 - f_1^2)^2}{(f^2 - f_0^2)^2 + \left(\frac{f f_0}{Q_a}\right)^2} \quad (2)$$

The term proportional to B is the relevant one, as it corresponds to the fluctuations of the cantilever induced by thermal or extra force noise, given by Eq. (1), converted into magnetic flux. The term proportional to A is the purely additive wideband noise of the SQUID. The last term, proportional to C arises because of the flux

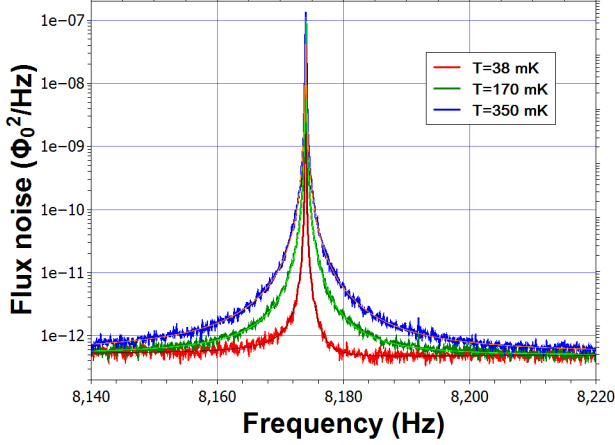


FIG. 2: Examples of averaged spectra at three representative temperatures, with the respective best fit with Eq. (2).

noise applied to the SQUID by the feedback electronics in order to compensate for the SQUID additive wideband noise. This flux noise induces a current J circulating in the SQUID through the finite responsivity $J_\Phi = dJ/d\Phi$ [21], which eventually leads to an effective back-action on the cantilever. The transfer function of this mechanism has been directly measured by injecting a calibration signal and features an antiresonance at $f = f_1$, with $f_1 - f_0 = 1.1$ Hz. The overall effect is a small asymmetric distortion of the Lorentzian peak.

All spectra have been checked to be fully consistent with Eq. (2) by means of χ^2 tests. All estimations of the SQUID parameters A and C are consistent with each other and do not depend significantly on temperature. This is consistent with previous noise measurements on the same type of SQUID [24] which have shown that the SQUID noise temperature is saturated by hot electron effect [25] for $T < 400$ mK. In fact, all measurements shown here are performed at $T < 350$ mK.

Fig. 3 shows the measured symmetric amplitude B of the Lorentzian noise as function of the bath temperature. The uncertainty on the estimation of B is remarkably low, of the order of 1%. The x -error bar, dominated by the uncertainty on Q , is thus significant. The data agree with a linear behaviour over the whole T/Q range. A weighted linear fit $B_0 + B_1 T/Q$ yields the intercept $B_0 = (1.20 \pm 0.14) \times 10^{-19} \Phi_0^2/\text{Hz}$ and the slope $B_1 = (0.293 \pm 0.002) \times 10^{-19} \Phi_0^2/(\text{nK} \cdot \text{Hz})$. We exploit the linear dependence on T/Q to infer the actual coupling between cantilever and SQUID. Given Eq. (1) and Eq. (2) we can express the thermal slope B_1 as:

$$B_1 = \frac{4k_B}{\omega_0} \frac{\Phi_x^2}{k} \quad (3)$$

where $\Phi_x = d\Phi/dx$ is the displacement to flux transduction factor. The measured coupling factor $\Phi_x^2/k \simeq 0.117$

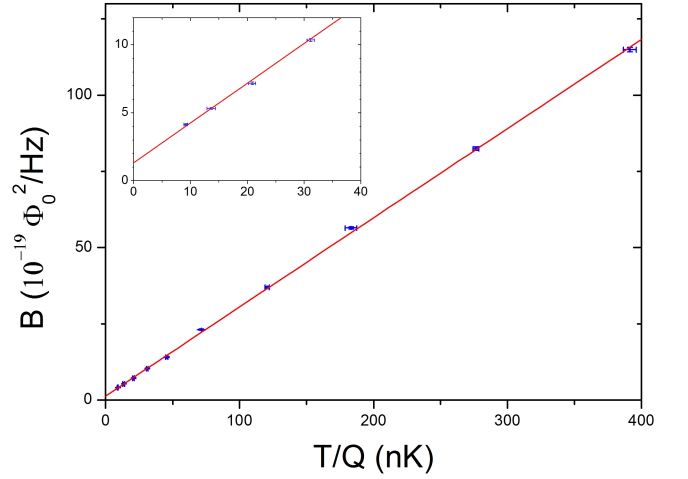


FIG. 3: Symmetric amplitude of the Lorentzian noise B , as measured by the SQUID, as function of the ratio T/Q , together with the best linear fit. In the inset, the data at the lowest T/Q are zoomed in order to highlight the nonzero intercept of the fit.

pH has the dimension of an inductance. The finite intercept, clearly visible in the inset of Fig. 3 implies that the data are not compatible with a pure thermal noise behavior, and a nonthermal excess noise is present. The corresponding force noise is $S_{f0}^{1/2} = (1.3 \pm 0.1) \text{ aN}/\sqrt{\text{Hz}}$.

Let us discuss possible physical sources of this excess noise. Based on standard Clarke-Tesche theory [27], we expect a significant intrinsic back-action force from the noise in the current circulating in the SQUID loop, with spectral density S_J . Circulating current couples a force noise to the cantilever with spectral density $S_{F,BA} = S_J F_J^2$. Because of reciprocity, the backward current-to-force factor $F_J = dF/dJ$ must be equal to the forward displacement-to-flux factor Φ_x [26]. The back-action noise leads then to a finite intercept in the data:

$$B_{0,BA} = S_J \left(\frac{\Phi_x^2}{k} \right)^2 \quad (4)$$

Because of the quadratic dependence on Φ_x^2/k , back-action noise can be easily discriminated from other noise sources by changing the coupling factor. Equivalently, we note that for an external force noise acting on the resonator, the ratio B_0/B_1 is independent of the coupling, and therefore of B_1 , as both terms scale with the coupling. In contrast, according to Eq. (4) the ratio $B_{0,BA}/B_1$ is proportional to B_1 .

We take advantage of this property by repeating all measurements at a different cantilever position, and effective coupling increased by a factor of 3. We observe again a linear behavior in very good agreement with the experimental data with $B_0 = (4.35 \pm 0.3) \times 10^{-19} \Phi_0^2/\text{Hz}$ and $B_1 = (0.869 \pm 0.007) \times 10^{-19} \Phi_0^2/(\text{nK} \cdot \text{Hz})$. However, the ratio B_0/B_1 is only slightly increased from

(4.2 ± 0.5) nK to (5.0 ± 0.3) nK. This clearly indicates that most of the observed excess noise cannot be attributed to SQUID back-action. From the observed small increase of B_0/B_1 we can estimate the equivalent noise spectrum S_J and compare it with the theoretical prediction $S_J = \gamma k_B T_{SQ} / R_{SQ}$ of the Clarke-Tesche model [27]. Here $R_{SQ} = 8 \Omega$ and $T_{SQ} = 400$ mK are the measured shunt resistor and the estimated saturation temperature. Comparison with experimental data gives $\gamma = 5 \pm 5$, essentially consistent with the theoretical value $\gamma = 11$ predicted for an optimized SQUID.

In order to investigate possible effects of vibrational noise from the refrigerator or from the outside world, we have repeated the measurements by keeping the pulse tube switched on. The actual input mechanical noise provided by the pulse tube in our systems is known to be 2-3 orders of magnitude larger than the background noise when the pulse tube is off. However, while the measured spectra with pulse tube on are significantly dirtier, there is no significant increase of the B parameter obtained by the fit. This confirms that the mechanical suspensions are working well within design specifications, and suggests that vibrational noise is not the source of the observed excess noise. We also ruled out noise from the ^3He flow by switching off the circulation pump.

As the ferromagnetic microsphere is magnetized, an external magnetic field noise could be also held responsible for anomalous force driving the cantilever. Let us assume an environmental magnetic noise B_n with direction along the cantilever length and negligible spatial dependence over the magnetic sphere volume. B_n would couple a torque μB_n , where $\mu \simeq 5 \times 10^{-9}$ J/T is the microsphere magnetic moment, which translates into an effective force noise $\mu B_n / l$, where l is the effective length of the cantilever. Under these assumptions, the observed excess force noise would result from a magnetic field noise B_n with spectral density 1×10^{-13} T/ $\sqrt{\text{Hz}}$. Such noise is typical of an unshielded environment at kHz frequency, but is unrealistically large for a shielded environment. The walls of the copper box hosting the cantilevers are about 20 times thicker than the penetration depth at the cantilever frequency, thus providing an attenuation of external magnetic fields by many orders of magnitude. Thermal magnetic noise from eddy currents in the walls or other elements inside the box is estimated to be largely negligible. In any case, it would appear as thermal noise, so it cannot be invoked to explain the observed nonthermal excess noise.

Other explanations may be considered, which require much longer and time consuming measurements to be tested. For instance, we may be observing thermomechanical noise, but the effective temperature of the noise source (or part of it) may be higher than the one of the thermal bath because of thermal gradients along the cantilever. In this case one would expect to observe saturation effects, as observed in [17] rather than a linear

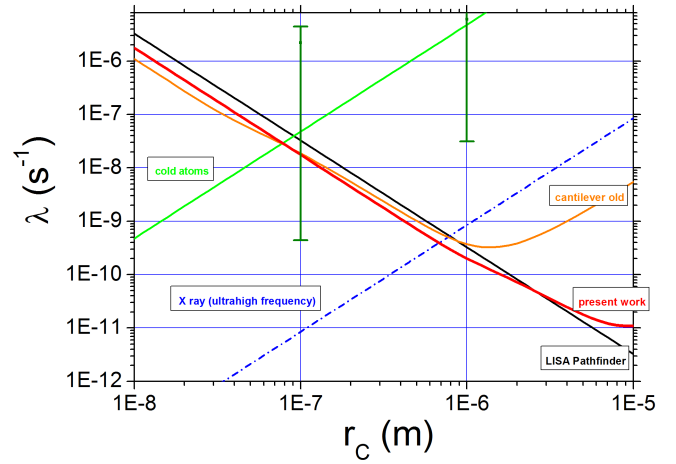


FIG. 4: Exclusion plot in the $\lambda - r_C$ plane based on our experimental data, compared with the best experimental upper bounds reported so far and with the proposed theoretical lower bound proposed by Adler [5] represented by the two vertical bars. Continuous thick (red) curve: upper limit on the CSL collapse rate λ , as function of the characteristic length r_C . The other thin lines represent upper limits from labeled experiments: previous cantilever experiment (orange line) [17], LISA Pathfinder (black line) [19], cold atoms (green line) [18] and X-ray spontaneous emission (dashed blue line) [20].

behaviour with a fixed intercept. Very accurate refined measurements with larger number of points may reveal such deviations from linear behaviour. On the theoretical side, we have performed simple thermal modeling of the cantilever. The power dissipated in the magnet by eddy currents induced by SQUID Josephson radiation is estimated of the order of 1 fW, and would cause a temperature gradient between the magnet and the cantilever base smaller than 1 mK in the temperature range explored by this experiment.

Finally, let us compare our results with the predictions of the CSL model. By using the same method discussed in Ref.[17], we can convert the observed excess noise into an upper bound on the CSL collapse rate λ as a function of r_C . The experimental upper limit on λ is shown in Fig. 4 and is significantly improved compared to previous experiments for $10^{-7} \text{ m} < r_C < 2 \times 10^{-6} \text{ m}$. This implies that the observed noise is in principle consistent with the effect of CSL, as it could not have been detected by previous experiments. Inversely, if the observed excess noise were not related to CSL, its identification and elimination would improve the bound by a factor of 10, thereby essentially ruling out Adler proposal.

In conclusion, we have improved the upper bounds on the CSL collapse rate in the r_C interval $10^{-7} \text{ m} < r_C < 2 \times 10^{-6} \text{ m}$. In contrast with previous cantilever measurements the new experiment features an excess noise, in principle compatible with the CSL Adler model [5]. Several physical mechanisms able to explain the observed

excess noise have been ruled out. Further investigations are needed in order to probe other possible explanations. Above all, this experiment neatly illustrates the fundamental challenge of collapse models testing. Negative results are robust, but positive claims require extremely careful and systematic work in order to exclude any conceivable alternative physical explanation.

* Electronic address: andrea.mistervin@gmail.com

- [1] G.C. Ghirardi, A. Rimini, and T. Weber, *Phys. Rev. D* **34**, 470 (1986).
- [2] G.C. Ghirardi, P. Pearle, and A. Rimini, *Phys. Rev. A* **42**, 78 (1990); G. C. Ghirardi, R. Grassi, and F. Benatti, *Found. Phys.* **25**, 5 (1995).
- [3] A. Bassi, and G. C. Ghirardi, *Phys. Rep.* **379**, 257 (2003).
- [4] A. Bassi, K. Lochan, S. Satin, T. P. Singh, and H. Ulbricht, *Rev. Mod. Phys.* **85**, 471 (2013).
- [5] S.L. Adler, *J. Phys. A* **40**, 2935 (2007).
- [6] K. Hornberger, S. Gerlich, P. Haslinger, S. Nimmrichter and M. Arndt, *Rev. Mod. Phys.* **84**, 157 (2012).
- [7] T. Juffmann, H. Ulbricht and M. Arndt, *Rep. Prog. Phys.* **76**, 086402 (2013).
- [8] M. Arndt and K. Hornberger, *Nat. Phys.* **10**, 271 (2014).
- [9] B. Collett and P. Pearle, *Found. Phys.* **33**, 1495 (2003).
- [10] S.L. Adler, *J. Phys. A* **38**, 2729 (2005).
- [11] A. Bassi, E. Ippoliti, S.L. Adler, *Phys. Rev. Lett.* **94**, 030401 (2005).
- [12] M. Bahrani, M. Paternostro, A. Bassi, and H. Ulbricht, *Phys. Rev. Lett.* **112**, 210404 (2014).
- [13] S. Nimmrichter, K. Hornberger, and K. Hammerer, *Phys. Rev. Lett.* **113**, 020405 (2014).
- [14] L. Diosi, *Phys. Rev. Lett.* **114**, 050403 (2015).
- [15] D. Goldwater, M. Paternostro, and P.F. Barker, *Phys. Rev. A* **94**, 010104 (2016).
- [16] J. Li, S. Zippilli, J. Zhang, and D. Vitali, *Phys. Rev. A* **93**, 050102 (2016).
- [17] A. Vinante, M. Bahrani, A. Bassi, O. Usenko, G. Wijts, T.H. Oosterkamp, *Phys. Rev. Lett.* **116**, 069402 (2016).
- [18] M. Bilardello, S. Donadi, A. Vinante, and A. Bassi, *Physica A* **462**, 764 (2016).
- [19] M. Carlesso, A. Bassi, P. Falferi, and A. Vinante, arXiv:1606.04581; B. Helou, B. Slagmolen, D.E. McClelland, and Y. Chen, arXiv:1606.03637.
- [20] C. Curceanu, B.C. Hiesmayr, and K. Piscicchia, *J. Adv. Phys.* **4**, 263 (2015).
- [21] C. Hilbert and J. Clarke, *J. Low Temp. Phys.* **61**, 237 (1985).
- [22] A. Vinante and P. Falferi, *Phys. Rev. Lett.* **111**, 207203 (2013).
- [23] A.D. Fefferman, R.O. Pohl, A.T. Zehnder, and J.M. Parpia, *Phys. Rev. Lett.* **100**, 195501 (2008).
- [24] P. Falferi, M. Bonaldi, M. Cerdonio, R. Mezzena, G.A. Prodi, A. Vinante, and S. Vitale, *Appl. Phys. Lett.* **93**, 172506 (2008).
- [25] F.C. Wellstood, C. Urbina, and J. Clarke, *Phys. Rev. Lett.* **49**, 5942 (1994).
- [26] O. Usenko, A. Vinante, G. Wijts, T.H. Oosterkamp, *Appl. Phys. Lett.* **98**, 133105 (2011).
- [27] C.D. Tesche and J. Clarke, *J. Low Temp. Phys.* **37**, 397 (1979).